Article Identifier
DOI: 10.22032/dbt.58727
URN: urn:nbn:de:gbv:ilm1-2023isc-141:2

60th ILMENAU SCIENTIFIC COLLOQUIUM
Technische Universität Ilmenau, 4 – 8 September 2023
URN: urn:nbn:de:gbv:ilm1-2023isc:1

MACHINE LEARNING APPROACH TO EIT IMAGE RECONSTRUCTION OF THE HUMAN FOREARM SECTION FOR DIFFERENT HAND SIGNS

Hayat Alasasfeh, Mariem Hafsa, Oumaima Bader, and Olfa Kanoun

Professorship of Measurement and Sensor Technology, Technische Universitat Chemnitz, Chemnitz, Germany
Université de Sousse, Ecole Nationale d'Ingénieurs de Sousse, LATIS- Laboratory of Advanced Technology and Intelligent Systems, 4023, Sousse, Tunisie;

ABSTRACT

Electrical impedance tomography (EIT) is an imaging technique used to reconstruct the conductivity of a target object from boundary voltages. In this study, we investigate suitable image reconstruction algorithms for EIT to enable the reconstruction of the conductivity distribution in the forearm section inferring muscle contractions at different hand signs. As EIT image reconstruction is an ill-posed inverse problem, the Gauss-Newton algorithm needs many iterations for the determination of suitable values of the regularization parameter and corresponding calculations of the Jacobian matrix. To reduce computational effort, we propose to use machine learning algorithms to directly reconstruct the EIT image. We explore the Radial Basis Neural Network (RBNN) and a one-dimensional Convolutional Neural Network (1D-CNN), which has been trained based on the measured EIT data for eight subjects, ten hand signs with ten trials. Both methods reach a low deviation at 0.0017 for RBNN and 0.0109 for CNN.

Index Terms **–** Image reconstruction, EIT, CNN, RBNN, Hand signs

1. INTRODUCTION

EIT is a non-invasive imaging technique that uses electrical currents to reconstruct the internal conductivity distribution of an object [1]. EIT is a radiation-free and cost-effective technology with applications in diverse fields such as medical imaging, geological exploration, industrial process monitoring, and environmental studies [2]. In EIT, low-amplitude electrical currents are injected between two electrodes on the surface of an object, and the resulting voltages are measured between other electrodes. These measurements are used to reconstruct a 2D or 3D image. Due to its portability and safety, EIT is increasingly being used in clinical filed such as monitoring lung ventilation, cerebral hemodynamics, breast cancer detection, and gesture recognition [3].

Hand signs (HSs) are a nonverbal communication approach in which the human hand expresses emotions or information. HSs are increasingly important in technology, particularly in human-computer interaction. With the proliferation of touchscreens, motion sensors, and augmented reality devices, it has become an intuitive and natural way to interact with technology [4]. In healthcare, it's being used to develop more intuitive and non-invasive interfaces for medical devices, enabling doctors and surgeons to control equipment and medical data. As such, the potential for revolutionizing the way to interact with technology and making it more accessible and intuitive for everyone lies within the development of HSs technology[5]. Different movements in the wrist move the internal muscle tissue and bones, which alters the conductivity distribution in the forearm. EIT can be used to reconstruct the conductivity distribution of the forearm because the EIT electrodes are unaffected by the external environment [6].

Intelligent Algorithms can also be an alternative to traditional reconstruction algorithms, which are always considered a regression problem [7]. Therefore, it can be classified into evolutionary methods and Neural Networks (NN). Evolutionary methods primarily include the Genetic Algorithm (GA) and Particle Swarm Optimization (PSO) [8][9] by lowering the root mean relative square error between simulated and measured data. The evolutionary algorithms are difficult to attain high precision, and the computation process is time-consuming. The NN method avoids the linearization of EIT image reconstruction because of the high nonlinear approximation ability [10]. The primary benefit of intelligent algorithms is that the Jacobian matrix solution was skipped entirely, removing the need for complex computations [11]. Due to the ill-posedness of the inverse problem of the EIT image reconstruction, the determination of appropriate values for the regularization parameter and corresponding calculations of the Jacobian matrix using the Gauss-Newton algorithm requires a significant number of iterations. To reduce computational effort, we propose to use machine learning algorithms to directly reconstruct the EIT image. We explore the Radial Basis Neural Network (RBNN), and a one-dimensional Convolutional Neural Network (1D-CNN), which have been trained using measured EIT data of eight subjects, 10 hand signs with 10 trials.

In our previous study [12], a geometric model of the human forearm was proposed to enhance the output of image reconstruction for different hand signs. This study aims to use intelligent tools as proof of concept for automatically reconstructing the internal conductivity of different gestures without referring to traditional algorithms. Traditional methods need more computation, and choosing a suitable regularization parameter is also challenging due to the complex nature of the human forearm. The input of the proposed network is a voltage vector, and the output is the corresponding conductivity vector. The possibility of using RBNN and 1D CNN for image reconstruction in EIT was applied to improve reconstruction as a regression problem.
This paper is structured as follows: Section II presents the employed methods, encompassing the dataset, reconstruction algorithms, and performance evaluation metrics. Section III provides the reconstruction results of experimental data. Lastly, section IV draws a conclusion and future work.

2. Methodology

2.1 Hand Sign Data

Data were collected from eight healthy subjects who measured each of the ten American sign numbers (0-9). To accommodate the high muscle density in the region, an 8-electrode EIT band was positioned below the elbow at approximately 30% of the total elbow length, as shown in Fig.1. During the experiments, commercial Ag/Agcl gel-based electrodes were used to reduce skin impedance. Additionally, subjects were instructed to abstain from consuming substances such as coffee or alcohol for at least 7 hours before the tests, as these can affect conductivity readings. Prior to each measurement, a 4-minute rest period was provided to ensure that subjects had sufficient recovery time. This rest period aimed to reduce the influence of muscular fatigue on subsequent measurements, thereby improving the reliability of the data collected. In order to stimulate the region of interest, an excitation signal with a frequency of 40 kHz and a current of 0.15 mA was applied to the subjects' forearms using an adjacent driven pattern. Subsequently, 40 boundary voltage measurements were obtained for each sign to reconstruct the corresponding conductivity.

Fig.1: EIT system with 8 electrode band around the forearm of a healthy subject [8]

2.2 Image Reconstruction

2.2.1 Gauss-Newton (GN)

EIT presents a challenging inverse problem characterized by nonlinearity and ill-posedness. To obtain an approximate solution, a minimization technique is employed. The objective function is minimized by evaluating the difference between the measured data and the predicted data. The GN algorithm is specifically designed to address the EIT inverse problem by seeking a solution denoted as the minimum of a sum of quadratic norms as in equation (1).

$$\hat{x} = \left|\left|z - jx\right|\right|^2 + \left|\left|x - x_0\right|\right|^2 \quad (1)$$

where z is the change in voltage, x is the change in conductivity value, and J Jacobian Matrix. By solving equation (2), a linear one-step inverse problem is defined as :

$$\mathrm{B} = (\mathrm{J}^T\mathrm{W}\mathrm{J} + \lambda^2\mathrm{R})^{-1}\,\mathrm{J}^T\mathrm{W} \quad (2)$$

Where B is the linear one-step inverse matrix, λ = σn/σx is the regularization parameter, J is a Jacobian matrix, J^T is the transpose of the Jacobian matrix, W is the weight of the matrix, and R is the regularization matrix. After that, the impedance tomography was obtained, which depicts the conductivity distribution in the reconstructed image. Newton's One-Step Error Reconstructor (NOSER) is a linearization-based approach where the R= diag (JT, J) is the regularization matrix used in the NOSER algorithm. The value of the exponent needs to be chosen correctly to keep a balance between stability and image contrast.

2.2.2 Radial Basis Neural Network (RBNN)

RBNN is a feedforward neural network; RBNN comprises three layers: input, hidden, and output. The number of hidden layers in RBNN is strictly restricted to one. This hidden layer is referred to as a feature vector. The input layer is a vector x = (Xl, X2, ..., XJ), j is the total number of elements in the hidden layer. The number of neurons in the hidden layer should be

greater than the number in the input layer. The radial basis function (RBF) is used as an activation function in the hidden layer. An RBNN differs from a standard neural network in that it uses RBF as its activation function precisely, a Gaussian RBF. The output layer includes a weighted sum of the neurons in the hidden layer that represent conductivity distribution equal to the number of triangles in the mesh. The mathematical calculations in the hidden layer are shown in equation 3, and the calculation in the output layer is described in equation 4. RBNN has excellent nonlinear mapping ability and global approximation ability. When applied to the nonlinear and ill-posed problem of EIT image reconstruction, the quality of the reconstructed image is expected to be improved.

$$f(x) = e^{-\beta||x-\mu_n||2} \tag{3}$$

$$y_m(x) = \sum_{n=1}^{N} w_{n,m}.f(x) \tag{4}$$

Where β is a parameter that controls gauss function width and how fast the function will decay, $\beta||x-\mu_n||2$ stands for Euclidean distance, x is the input, μ is the prototype vector, and yk is the output vector y (x) = (yl,y2, ...,ym). Voltage vector composed of 40 voltage measurements and Conductivity vector representing conductivity distribution as an output to the network. The following network parameters were set: The learning rate was set to 0.0001, and the batch size was set to 5. The number of iterations found to be the most effective was 170. The number of RBF layer neurons was set to 5000 and beta 1. Figure 2 shows the architecture of RBNN.

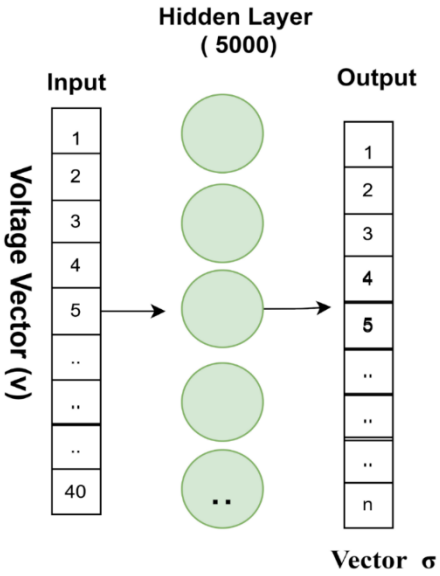

Fig.2: RBNN architecture.

2.2.3 Convolution Neural Network (CNN)

CNN is a class of deep neural networks, which has a significant advantage over the classical network in the automatic feature extraction ability. When using deep learning techniques in EIT, the following steps must be completed: collecting data, choosing an appropriate network, optimizing the network, and determining network parameters. 1D voltage data is used as input to 1D-CNN, and conductivity distribution as network output. The convolutional layers convolve around their input to extract features, max pooling, which calculates the maximum value. Dropout works by probabilistically eliminating a neuron from designated layers during

training or removing a certain connection to prevent overfitting and improves the training speed significantly. Flatten layer is the one in between the convolutional and fully connected layers. It is called "flatten" because it transforms the matrix of features into a representative vector that forms the input of the fully connected neural network. A dense layer means that each neuron is connected to all the neurons in the previous layer, so it is also called Fully connected.
The input to 1D-CNN is a voltage vector with the size of 40x1. This model consists of three convolutional layers followed by three max-pooling layers, flatten layer, and three dense layers. To avoid overfitting batch normalization after each pooling layer and dropout layer with 50% after each dense layer have been added. The output layer is a conductivity vector with 2428 elements for experimental data. Moreover, the sigmoid activation function was used in the output layers and the Relu activation function in the convolutional and dense layers. The convolution layers with padding = "same" and stride = 1. The sizes of the three convolutional kernels are 1 × 64 × 3, 1 × 32 × 3, and 1 × 16 × 3, as shown in Fig.3. Adam optimizer was used to calculate and update the parameters in the model training. The initial learning rate was set to 0.001, the batch size was 5, and the number of epochs was 1000. We also implement callbacks, particularly early stopping to stop the training process when the loss doesn't change, and the learning rate scheduler (LRS) schedules the learning rate during training. In LRS takes a parameter called step decay(late) and its defined as:

$$lrate = initial_{lrate} * \left(drop^{\lfloor (x) \rfloor}\right) \tag{5}$$

$$(x = 1 + epoch)/epochs\_drop \tag{6}$$

⌊x⌋ returns the floor of (x), the largest integer not greater than x. The drop = 0.5, epochs drop = 10.0 The patience in early stopping was set to 15.

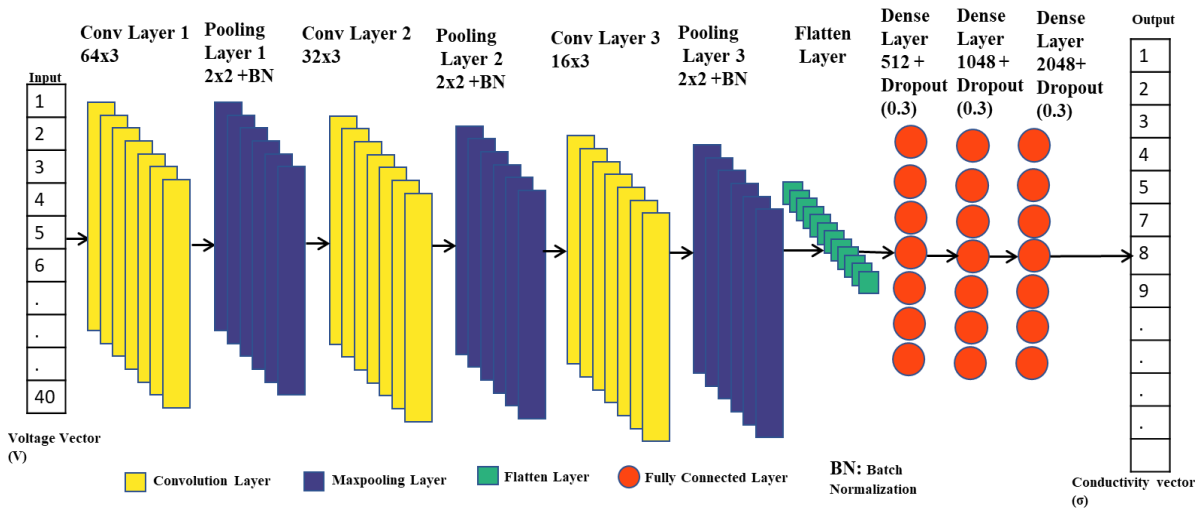

Fig.3: 1D-CNN architecture

2.2.4 Performance Evaluation

Mean square error (MSE) and image correlation coefficient (ICC) are used to evaluate the reconstruction performance. The mathematical equations for MSE and ICC are shown in equation 7 and equation 8.

$$\text{MSE} = \frac{\sum_{i=1}^{n} ||\sigma^* - \sigma||_2}{n} \tag{7}$$

$$\mathrm{ICC} = \frac{\sum_{i=1}^{n}(\sigma^* - \overline{\sigma^*})(\sigma - \bar{\sigma})}{n} \tag{8}$$

Where, σ* **is** the actual conductivity, σ predicted conductivity and number of data points, $\overline{\boldsymbol{\sigma}^*}$ average of actual conductivity and $\overline{\boldsymbol{\sigma}}$ Average of predicated conductivity. MSE; The lower the value, the better, and 0 means the perfect model, which means the reconstructed and ground truth image are identical. Whereas ICC; the higher the value, the better, and 1 means the model is perfect when the ideal and reconstructed images are identical.

3. Results

3.1 Radial Basis Neural Network (RBNN)

The reconstruction results from GN in our previous study [12] were assumed to be an input to the network. However, choosing a suitable regularization parameter is also challenging due to the human forearm complex nature, which affect the results. The loss curve of the training and validation data are shown in Fig. 4. The X-axis depicts the number of existing epochs, while the Y-axis represents a loss. The blue curve shows how loss varies with testing data, whereas the orange curve depicts how loss changes with training data. As the iteration times increase, the loss curves of the training and testing show a similar pattern. MSE and ICC are used to evaluate the performance of the proposed method as listed in table 1. During the training phase, they converge to a loss of 0.01, and ICC is 0.88 suggesting that the network high performance model, and the error is low.

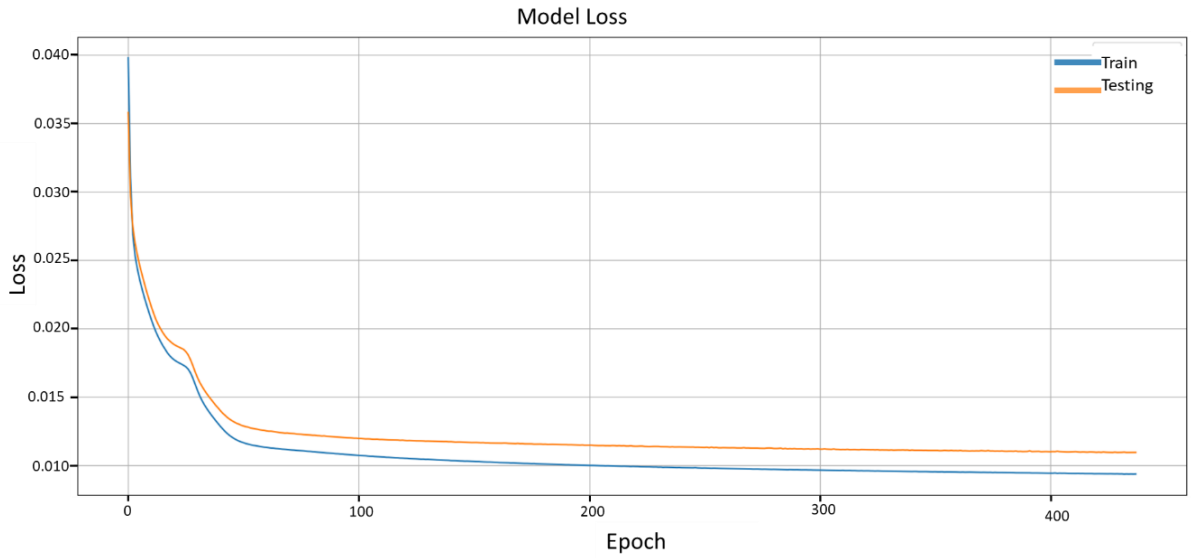

Fig.4: Loss curve for RBNN

3.2 Convolution Neural Network (CNN)

The loss curve for training and testing data using CNN is shown in Fig. 5. The curve of training and testing datasets follows a similar pattern as the iteration times grow. They converge to a loss of 0.0017 during the training phase, indicating a high-performance network. MSE and ICC were used to implement the comparison. To demonstrate the results of each image reconstruction method, we chose different hand signs, as shown in Fig.6. RBNN and CNN showed similar performance and predict similar conductivity in GN except that the error in CNN is less than the error in RBNN. The loss for RBNN is 0.0109, whereas, for CNN, it is 0.0017. The ICC value for RBNN is 0.88, while for CNN, it is 0.93. Furthermore, CNN demands less time compared to RBNN which necessitate a higher number of epochs to

complete the process. This assertion is supported by the observation that the ICC value is higher and the MSE value is lower in the CNN model as shown in table 1. As a result, the suggested CNN approach has a higher prediction accuracy, and the quality of the reconstructed images is improved.

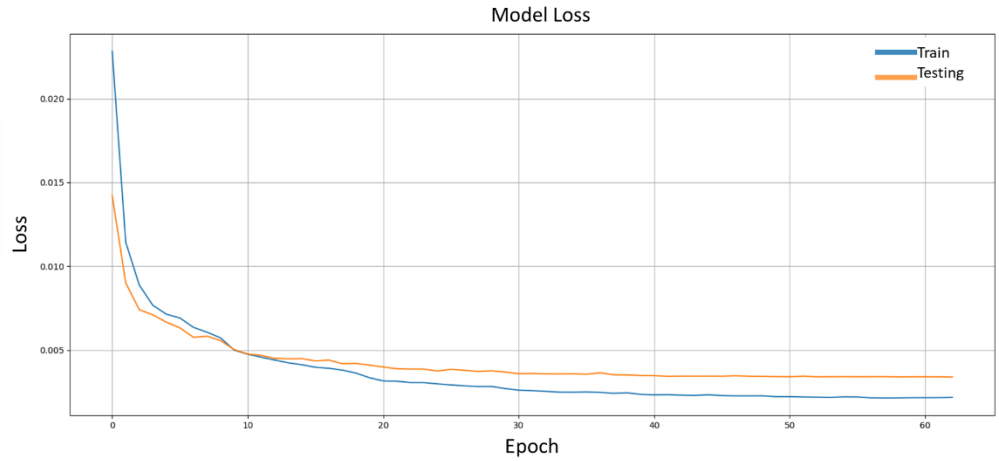

Fig.5: Loss curve for 1D-CNN

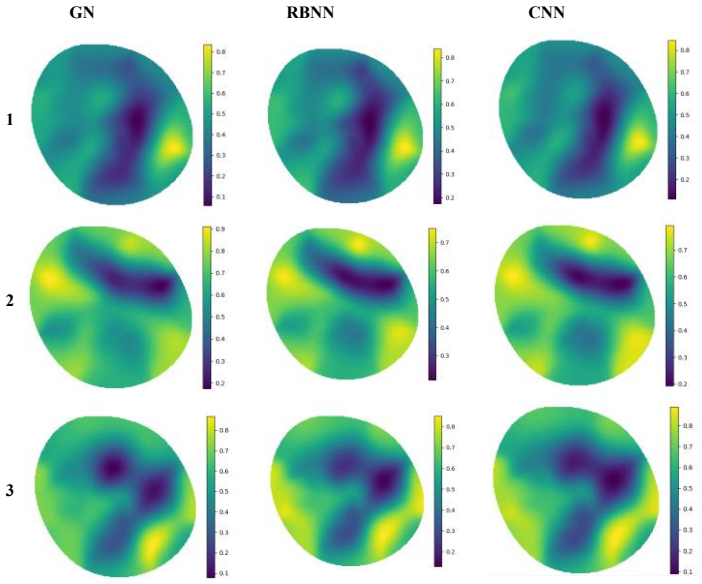

Fig.6: Reconstruction using the algorithms GN, RBNN, and CNN

Table 1: MSE and ICC values for RBNN and CNN

	RBNN		CNN	
	MSE	ICC	MSE	ICC
Training	0.0093	0.92	0.0008	0.96
Testing	0.0109	0.88	0.0017	0.93

Conclusion

In this study, neural networks were utilized to reconstruct the internal conductivity of the human forearm using experimental data. The outcomes demonstrated the neural network capability to predict and reconstruct various signs without need for conventional algorithms procedures such as Jacobian calculations and regularization setting, which are computationally complex. This preliminary work serves as a foundation for utilizing machine learning algorithms in real-world EIT systems, with a recognition that further enhancements are necessary. Subsequent research will focus on incorporating additional reconstruction and expanding the dataset to improve the reconstruction quality.

ACKNOWLEDGMENT
The authors would like to thank the DAAD for the support through the project " , Promotion of Higher Education in Biomedical Engineering, grant number :57612192".

REFERENCES

[1] Y. Wu, F. F. Hanzaee, D. Jiang, R. H. Bayford, and A. Demosthenous, "Electrical Impedance Tomography for Biomedical Applications: Circuits and Systems Review," *IEEE Open Journal of Circuits and Systems*, vol. 2, pp. 380–397, Apr. 2021, doi: 10.1109/OJCAS.2021.3075302.

[2] T. K. Bera, "Applications of Electrical Impedance Tomography (EIT): A Short Review", doi: 10.1088/1757-899X/331/1/012004.

[3] B. Lobo, C. Hermosa, A. Abella, and F. Gordo, "Electrical impedance tomography," *Ann Transl Med*, vol. 6, no. 2, pp. 26–26, Jan. 2018, doi: 10.21037/ATM.2017.12.06.

[4] M. J. Cheok, Z. Omar, and M. H. Jaward, "A review of hand gesture and sign language recognition techniques," *International Journal of Machine Learning and Cybernetics*, vol. 10, no. 1, pp. 131–153, Jan. 2019, doi: 10.1007/S13042-017-0705-5/TABLES/5.

[5] M. Oudah, A. Al-Naji, and J. Chahl, "Hand Gesture Recognition Based on Computer Vision: A Review of Techniques," *Journal of Imaging 2020, Vol. 6, Page 73*, vol. 6, no. 8, p. 73, Jul. 2020, doi: 10.3390/JIMAGING6080073.

[6] B. Ben Atitallah *et al.*, "Hand Sign Recognition System Based on EIT Imaging and Robust CNN Classification," *IEEE Sens J*, vol. 22, no. 2, pp. 1729–1737, Jan. 2022, doi: 10.1109/JSEN.2021.3130982.

[7] T. Zhang *et al.*, "Advances of deep learning in electrical impedance tomography image reconstruction," *Front Bioeng Biotechnol*, vol. 10, Dec. 2022, doi: 10.3389/FBIOE.2022.1019531.

[8] M. Hafsa, B. Ben Atitallah, T. Ben Salah, N. Essoukri Ben Amara, and O. Kanoun, "Ein genetischer Algorithmus für die Bildrekonstruktion in der elektrischen Impedanz Tomographie zur Gestenerkennung," *Technisches Messen*, vol. 89, no. 5, pp. 310–327, May 2022, doi: 10.1515/TEME-2021-0126/MACHINEREADABLECITATION/RIS.

[9] O. Kahouli, M. Hafsa, H. Hellara, I. E. Bennour, N. E. Ben Amara, and O. Kanoun, "Enhanced Particle Swarm Optimization Algorithm for EIT Image Reconstruction," *Proceedings of International Workshop on Impedance Spectroscopy, IWIS 2022*, pp. 111–116, 2022, doi: 10.1109/IWIS57888.2022.9975123.

[10] G. Yao, T. Lei, and J. Zhong, "A review of Convolutional-Neural-Network-based action recognition," *Pattern Recognit Lett*, vol. 118, pp. 14–22, Feb. 2019, doi: 10.1016/J.PATREC.2018.05.018.

[11] X. Li *et al.*, "An image reconstruction framework based on deep neural network for electrical impedance tomography," *Proceedings - International Conference on Image Processing, ICIP*, vol. 2017-September, pp. 3585–3589, Feb. 2018, doi: 10.1109/ICIP.2017.8296950.

[12] H. Alasasfeh, M. Hafsa, O. Bader, M. Ibbini, S. Hasan, and O. Kanoun, "Electrical Impedance Tomography Image Reconstruction with apriori Knowledge for Gesture Recognition," *2022 19th IEEE International Multi-Conference on Systems, Signals and Devices, SSD 2022, pp. 1770–1775, 2022, doi: 10.1109/SSD54932.2022.9955849.*

